

## MAXIMUM POWER TRACKING FOR PV SYSTEMS

G. Vivekananda\*

V. Krishnanaik\*\*

### ABSTRACT

In this paper photo voltaic (PV) electricity is one of the best options for most important and ecological future energy requirements of the world. Organic photovoltaic (OPV) cells are hopeful views for common renewable energy unpaid to light weight, low cost, and flexibility. An organic solar cell or organic photovoltaic (OPV) cell is a photovoltaic cell that uses organic electronics—a branch of electronics that deals with conductive organic polymers or small organic molecules for light absorption and charge transport. The plastic used in OPV cells has low production costs in high volumes. Combined with the flexibility of organic molecules, OPV cells are potentially cost-effective for photovoltaic applications. Solar photovoltaic (PV) panels are a great source of renewable energy generation. The biggest problem with solar systems is relatively low efficiency and high cost. In this research work hopes to alleviate this problem by using novel power electronic converter and control designs. An electronic DC/DC converter, called “Quasi-Double-Boost DC/DC Converter,” is designed for a Solar PV system. A Maximum Power Point Tracking (MPPT) algorithm is implemented through this converter. This algorithm allows the PV system to work at its highest efficiency. Different current sensing and sensorless technologies used with the converter for the MPPT algorithm are offered and tested. Design aspects of the system and components will be discussed. Results from simulations and experiments will be presented. These results will show that the proposed converter and MPPT control algorithm improves overall PV system efficiency without adding much additional cost.

**Keywords :** Maximum Power, PV System, MPPT, DC, System Layout, PV panels, I-V Curves, CCM, DCM

\* Asst. Professor, Department of Electrical & Computer Engineering, Aksum University

\*\* PhD Research Scholar of Mewar University, Dept of ECE, Mewar University, Chittorgarh, Rajashtan, India,

## 1. INTRODUCTION

The past few years have been filled with news of fuel price hikes, oil spills, and concerns of global warming. One of the few positives that can be taken from this is that it is changing the average person's mindset towards renewable energy. People are finding the benefits of having their own renewable energy system more attractive than they ever have before. The biggest form of renewable energy to benefit from this is solar PV systems because of their many merits, such as cleanliness and relative lack of noise or movement, as well as their ease of installation and integration when compared to wind turbines. However, the output power of a PV panel is largely determined by the solar irradiation and the temperature of the panel. At a certain weather condition, the output power of a PV panel depends on the terminal voltage of the system. To maximize the power output of the PV system, a high-efficiency, low-cost DC/DC converter with an appropriate maximum power point tracking (MPPT) algorithm is commonly employed to control the terminal voltage of the PV system at optimal values in various solar radiation conditions. There are three main DC/DC converter technologies used with most PV systems (Bernardo, 2009; Morales-Saldana, 2006; Mrabti, 2009; Nabulsi, 2009; Shanthi, 2007). The first of these converters is the buck converter (Bernardo, 2009; Mrabti, 2009). Buck converters are step-down converters that output a voltage lower than the voltage that is input to the converter. The standard buck converter has an output that is equivalent to the input voltage multiplied by the duty cycle or

$$V_{out} = D * V_{in} \dots\dots\dots 1.1$$

Buck converters work for low voltage applications. They can be implemented in MPPT algorithms (Bernardo, 2009), as long as the PV panels output voltage is greater than the voltage required by the load. To maximize the efficiency of the PV panel from near zero to the maximum output, the entire range of the duty cycle needs to be used for the implementation of the MPPT algorithm. The second commonly used converter in PV systems is a boost converter (Shanthi, 2007). Boost converters are step-up converters that output a voltage higher than the voltage that is input to the converter. The standard boost converter has an output that is equivalent to the input voltage divided by the duty cycle.

$$V_{out} = V_{in} / (1 - D) \dots\dots\dots 1.2$$

Basic boost converters work well with the MPPT control as long as the load can accept a voltage from the minimum output of the PV panel all the way up a certain value (e.g., 5 times) subject to

practical limits of the duty cycle (e.g., 80%). However, in many applications, a high boost ratio is required for the DC/DC converter to connect the low-voltage PV panel to a relatively high-voltage load or power grid. This cannot be satisfied by using basic boost converters. The third commonly used converter in solar PV systems is a cascaded boost converter (Morales-Saldana, 2006; Nabulsi, 2009). Cascaded boost converters have an output that is equivalent to the input voltage divided by the duty cycle to the  $n$ th power, where  $n$  refers to the number of boost converters that are cascaded.

$$V_{out} = V_{in} / (1-D)^n \dots\dots\dots 1.3$$

Cascaded boost converters work well in applications that require high voltage boost ratios. One problem with both the boost and the cascaded boost converters is the oscillations and relative instability under changing and startup conditions as shown in (Rensburg, 2008). In order to utilize the potential with any of these converters in a PV system, the converter needs to be controlled by a MPPT algorithm. Various MPPT algorithms (Hua, 1998; Hussein, 1995; Koutroulis, 2001; Pan, 1999) have been proposed based on power measurements, including the hill-climbing (HC) method (Koutroulis, 2001), perturb-and-observe (P&O) method (Hua, 1998), and incremental conductance (IncCond) method (Hussein, 1995). The HC and P&O methods achieve the same fundamental thought in different ways (Salas, 2006). These two algorithms are widely used because of their simplicity; however they can fail under rapidly changing atmospheric conditions. The incremental conductance method can track the maximum power point (MPP) more accurately than the HC and P&O algorithms can, however it is relatively complicated to implement. Every addition, converter and MPPT algorithm add additional cost to the entire PV system. However the cost is minimal compared to the PV panels and can usually be offset by improved efficiency. Improving efficiency is the easiest way to cut cost with a PV system. A good MPPT algorithm and a high efficiency converter are a must to improve efficiency but should not be the only changes to the standard setup. One should also employ higher output voltages to lower line losses and allow for more efficient AC conversion. The second easiest way to improve overall system cost is in the components themselves. A higher and more stable line voltage will mean smaller AC inverters with grid tie systems that will not need any boosting capabilities at all. The removal of expensive components such as current sensors also helps to keep cost at a minimum and improves the system reliability. The system needs to be robust enough that when the consumer wants to expand their energy production by adding more panels, they don't need to replace their

entire system. The DC/DC converter and MPPT control algorithm proposed in this work will implement all of these improvements in hopes creating a highly efficient, low-cost, and highly reliable solar PV system for clean and renewable power generation.

## 2. SYSTEM LAYOUT

The overall PV system layout can be seen in Figure 1. The system consists of a PV panel or panels, a quasi-double-boost DC/DC converter, a MPPT control algorithm and some sort of load.

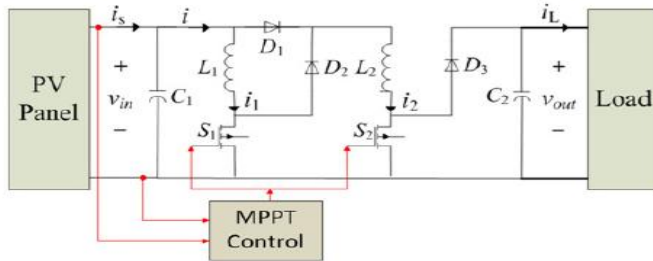


Figure 1. The layout of the overall PV System

### 2.1 The PV Panel

PV panels generate electricity through what is called the “Photovoltaic Effect” (Wenham, 2009). In the simplest form the Photovoltaic Effect can be described as follows: Light particles called photons are constantly emitted from the Sun. This can be seen by the brightness on a sunny day when many of these particles make it to earth’s surface. The effect comes into play when these particles hit a PV material, such as a solar cell. When the photons impact this material it excites the atoms within the material, which causes an electron-hole pair to form. A band gap built into the material causes the electron to move along a certain predefined path. This electron-hole pair creation happens many times over, throughout the panel. All of these flowing electrons generate a current that is directed out of the panel to some type of load. Thus, the photovoltaic effect converts light into the more useful form of power, electricity. Solar cells output power in what is called an I-V curve. A typical I-V curve of a solar cell can be seen in Figure 2 (Wenham, 2009). This curve represents what the current output by the solar cell would be as the output voltage is varied and vice versa. Below the I-V curve, the P-V curve is also

shown in Figure 2. This curve can be easily obtained from the I-V curve through the equation  $P = V \times I$ .

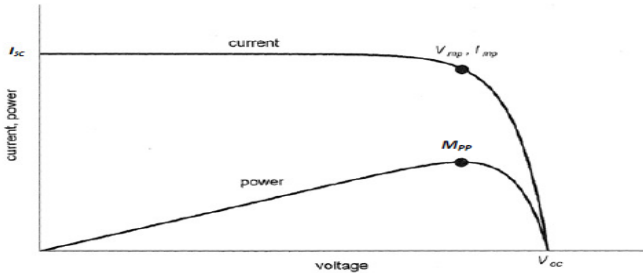


Figure2 : A rep I- V cure for a solar cell showing the MPP

There are three other important aspects of a solar cell also shown in Figure 2. The first two are the open circuit voltage ( $V_{oc}$ ) and the short circuit current ( $I_{sc}$ ) of the cell. The open circuit voltage is the voltage that is output to the cell terminals when the cell is exposed to light and there is no current flowing between the terminals. This is also the maximum voltage that can be produced by the cell, which makes knowing this number useful when designing a circuit or load to connect to the cell terminals. The short circuit current is the current that will flow when the cell is under light and the terminals are shorted together. This is the maximum current that can be output by the specific solar cell. The third important aspect of a solar cell is the MPP. This is the point where the cell is operating at maximum efficiency and outputting the highest power available. The MPP also has voltage at maximum power ( $V_{mp}$ ) and current at maximum power ( $I_{mp}$ ) points associated with it. The way these points move and change with the environmental conditions around the cell will be discussed in more detail later.

Each individual cell is relatively little in size and can only produce a small amount of power. The  $V_{oc}$  of an individual solar cell is usually approximately 0.6 V (Wenham, 2009). The cells become much more useful when combined in an array to create a PV panel. When connected together the cells properties add together to create an I-V curve that has the same appearance as that of an individual cell but is larger in magnitude. The cells in an array are usually connected in series to obtain a higher and more appropriate terminal voltage. The PV panels used in this research are BP Solar model SX 3175 (Appendix 1). Each panel consists of 72 individual solar cells connected in

series to obtain a rated power of 175 W, which corresponds to a maximum power current and voltage of 4.85 A and 36.1 V, respectively. The panel has an open circuit voltage of 43.6 V and a short-circuit current of 5.3 A.

### 2.2 Modeling of the PV Panel

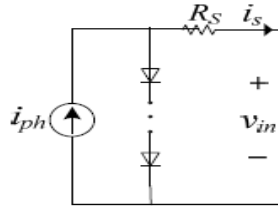


Figure 3: the PV Panel model

A PV panel model is developed using the work in (Tsai, 2008) as a starting point. The panel is modeled as a current source as shown in Figure 3 that follows equation 2-1

$$i = I_{ph} - I_S \sigma (\exp\{q(V_{in} + i \cdot R_S) / kTA\} - 1) \dots\dots\dots 2.1$$

where  $i$  is the PV panel output current;  $I_{ph}$  is photocurrent;  $I_S(T)$  is the reverse saturation current;  $q$  ( $= 1.6 \times 10^{-19}$ ) is an electron charge;  $V_{in}$  is the terminal voltage of the PV panel;  $R_S$  is the PV panel series resistance;  $A$  is the ideal factor of the PN junction of the PV diode, which varies in the range of [1, 2]; and  $k$  ( $= 1.38 \times 10^{-23} \text{ J/K}$ ) is the Boltzmann constant. The photo current is then found using equation 2-2.

$$I_{ph} = [I_{sc} + K_i(T - T_{ref})] \cdot \lambda \dots\dots\dots 2.2$$

where  $I_{sc}$  is the short circuit current provided by the PV panel at a reference temperature and an irradiance of  $1 \text{ kW/m}^2$ ;  $K_i$  ( $= 3 \text{ mA/}^\circ\text{C}$ ) is the temperature coefficient,  $\lambda$  is the solar irradiance in  $\text{kW/m}^2$ ; and  $T$  and  $T_{ref}$  are measured temperature and reference temperature, respectively. The output current is then

$$I_S(T) = I_S(T_{ref}) \exp\{K_s(T - T_{ref})\} \dots\dots\dots 2.3$$

where  $I_S(T_{ref})$  is the reverse saturation current ( $T_{ref} = 295 \text{ K}$ ) and  $K_s$  ( $\approx 0.072/^\circ\text{C}$ ) is the temperature coefficient of the PV panel.

### 2.3 The Quasi-Double-Boost DC/DC Converter

Many DC/DC converter topologies were considered prior to designing the system. Ultimately a double-boost DC/DC converter (Rensburg, 2008) was chosen because of the requirement for a high voltage regulation ratio (200/28) as well as the converter's output stability over the entire duty cycle range. As shown in Figure 1, the double-boost DC/DC converter consists of two inductors, two switches and three diodes. The boost function is achieved by switching the two switches simultaneously. However, the following analysis reveals that the voltage regulation ratio is not exactly double boost previously derived (Rensburg, 2008).

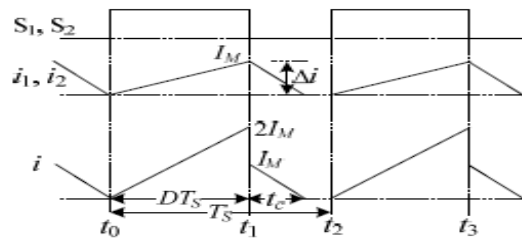


Figure 4. The current waveform in DCM mode.

The converter can work in a continuous current mode (CCM) or a discontinuous current mode (DCM). The DCM is studied since the CCM is a special case of the DCM. The waveforms in the DCM are shown in Figure 4, where S1 and S2 are the gate signals of the two switches; TS and D are the switching period and duty ratio of the DC/DC converter, respectively; tc is the duration that the inductor currents decrease to zero from the maximum value; and IM is the maximum inductor current. Neglecting the ripples of vin and vout, the following formula can be obtained for the switch on and off periods, respectively.

$$I_M = \frac{V_{in}DT_s}{L} \dots\dots\dots 2.4$$

$$V_{in} - V_{out} = -2L \frac{I_M}{t_c} \dots\dots\dots 2.5$$

where L1 = L2 = L; Vin and Vout are the average values of vin and vout, respectively. Then the voltage regulation ratio can be obtained from (2-4) and (2-5) as follows.

$$\frac{V_{out}}{V_{in}} = \frac{2DT_s + t_c}{t_c} \dots\dots\dots 2.6$$

The average value of the input current I in a period can be calculated as:

$$I = \left( D + \frac{t_c}{2T_s} \right) I_M \dots\dots\dots 2.7$$

According to the power conservation law,  $V_{in} \cdot I = P_{out}$ , then

$$\frac{V_{out} \times V_{out}}{R} = V_{in} \left( D + \frac{t_c}{2T_s} \right) I_M \dots\dots\dots 2.8$$

where R is the equivalent resistance of the load. Substituting (2-4) and (2-7) into (2-8), then

$$\frac{D + \frac{t_c}{2T_s}}{\frac{t_c}{2T_s} \times \frac{t_c}{2T_s}} = \frac{D \cdot T_s \cdot R}{L} \dots\dots\dots 2.9$$

The conduction time  $t_c$  can be derived from (2-9).

$$t_c = \frac{1 + \sqrt{1 + 4D^2 T_s \left( \frac{R}{L} \right)}}{D \left( \frac{R}{L} \right)} \dots\dots\dots 2.10$$

Equation (2-10) indicates that the conduction time during the switch off period is related with R, L, T, and D. The following formula can be obtained by substituting (2-10) into (2-6).

$$\frac{V_{out}}{V_{in}} = \frac{1 + \sqrt{1 + 4D^2 T_s \left( \frac{R}{L} \right)}}{2} \dots\dots\dots 2.11$$

Equation (2-11) indicates that in the DCM, the voltage ratio is not only determined by the duty ratio, but also determined by the output current and the inductance value. If the equivalent load resistance varies from time to time, the duty ratio should be changed to sustain the desired voltage gain.

When  $t_c = (1-D) T_s$ , the converter works in the critical mode, substituting  $t_c$  into (2-9), then the critical inductance  $L_c$  is:

$$L_c = \frac{D(1-D)^2 \cdot RT_s}{(1+D) \cdot 2} \dots\dots\dots 2.12$$



Equation (2-12) indicates that the critical inductance depends on the duty cycle and load. Equation (2-12) also indicates that there exist a supremum (i.e., the least upper bound) value  $L_M$  such that for any  $L > L_M$ , the circuit will work in the CCM for any duty ratios. This unique maximal critical inductance can be derived by setting the first derivative of  $L_C$  with respect to  $D$  as zero.

$$\frac{\partial L_C}{\partial D} = 0 \quad \dots\dots\dots 2.13$$

Then

$$L_M = 0.113 \cdot \frac{RT}{2} \quad \dots\dots\dots 2.14$$

Therefore, (2-14) can be used to design the inductor so that the circuit always works in the CCM when the load is fixed. On the other hand, if the inductance is fixed, then there exists a critical duty cycle ( $DC$ ), when  $D < DC$ , the converter works in the DCM; otherwise, the converter works in the CCM, in which (2-6) can be further simplified as:

$$\frac{V_{out}}{V_{in}} = \frac{1+D}{1-D} \quad \dots\dots\dots 2.15$$

Equation (2-15) indicates that the voltage regulation ratio is not simply twice that of the basic boost converter as claimed in (Rensburg, 2008). Thus, the original double-boost converter named in (Rensburg, 2008) is called the quasi-double-boost converter from here on.

### 3 THE MAXIMUM POWER POINT TRACKING ALGORITHM

The P&O algorithm is a relatively simple yet powerful method for MPPT. The algorithm is an iteration based approach to MPPT (Salas, 2006). A flowchart of the method can be seen in Figure 5. The first step in the P&O algorithm is to sense the current and voltage presently being output by the PV panel and use these values to calculate the power being output by the panel. The algorithm then compares the current power against the power from the previous iteration that has been stored in memory. If the algorithm is just in the first iteration the current power will be compared against some constant placed in the algorithm during programming. The system compares the difference between current and previous powers against a predefined constant.

This constant is placed within the algorithm to ensure that when the method has found the MPP of the PV panel, the duty cycle will remain constant until the conditions change enough to change the location of the MPP. If this step is not included the algorithm would constantly change the duty cycle, causing the operating point of the panel to move back and forth across the MPP. The movement across the MPP is an unwanted oscillation that can be disruptive to power flow and could also cause unwanted loss from not having the operating point right over the MPP at all times. The next step in the algorithm is determining whether the current power is greater than or less than the previous power. The answer to this tells the algorithm which branch of the flowchart to take next. No matter which direction the algorithm takes, the next step is to compare the voltages in the current and previous iterations. The voltage comparison tells the algorithm which side of the MPP the operating point is at thereby allowing the algorithm to adjust the duty cycle in the right direction, either a positive or negative addition to the current duty cycle. The final step of the method is to actually change the duty cycle being output to the converter, and wait for the converter to stabilize before starting the process all over again.

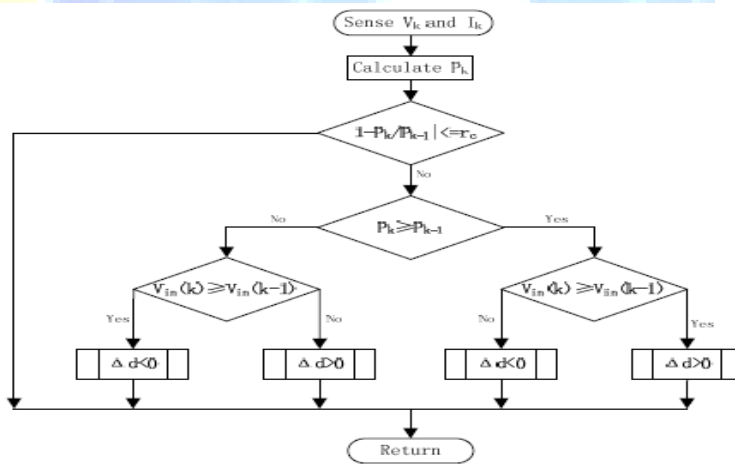


Figure 5. Flowchart

There are multiple ways to try to optimize the P&O algorithm. The first and most important is to choose the constants within the system carefully. The first constant ( $r_c$  in the flowchart) that tells the algorithm whether or not the MPP has changed, needs to be sized just right. It needs to be big enough to stop the oscillation effect once the MPP has been found but small enough to ensure that the algorithm will move to the correct point when the MPP changes even slightly. Another important constant to optimize is the amount the duty cycle changes ( $\Delta d$ ) with each perturbation. This

needs to be small enough to allow for a sufficient number of steps within the full duty cycle range. It is

also important to make this number small enough that when the MPP is reached one change won't be enough to throw it over the MPP causing the same oscillations that were avoided by sizing correctly. This also means that the amount of change in the duty cycle should be correlated with the first constant as well as. This all makes it sound

as though it would be best to have  $\Delta d$  as small as possible, but this would also cause problems. The system needs to be able to respond to rapid changes in the environment, such as cloud cover. If a cloud suddenly shades part of the panel the algorithm should be able to quickly account for the change in MPP and move the operating point to the new MPP. Having the amount of change in the duty cycle per iteration very small would mean that it would take a great number of iterations to reach the new MPP. Every iteration where the panel is not operating at the MPP can be considered a loss in power. Therefore it is important to have  $\Delta d$  be large enough to allow the algorithm to converge to a new MPP quickly. This shows that there is a large trade off between speed and efficiency with this algorithm. The algorithm in use here increases or decreases the duty cycle by 0.125% per iteration. The last main way to optimize this algorithm is to change the time between when one iteration ends and the next one begins. There needs to be enough time between the iterations to be sure that the converter or panel has reached a steady state after a variation in duty cycle. If there is not enough time the power calculation may be being made from fluctuating voltage and currents. The fluctuations would cause the calculated power to be wrong, which could make the rest of the algorithm change the duty cycle in the wrong direction. Here again careful decisions need to be made though, because if the time between iterations is too long then there will be convergence issues with the system under rapidly changing conditions.

#### 4. RESULTS

Simulation studies are carried out in MATLAB Simulink to validate the converter and MPPT control for a PV system as is presented in Appendix 2.

#### 4.1 Validation of the PV Panel Model

The PV panel model is firstly tested to make sure it is accurate. The results from the first test can be seen in Figure 11. In this test the I-V curves are found after different levels of solar irradiance were applied to the model. It can be seen here that while the voltage remains nearly the same, the current changes greatly with varying irradiance. In the second test, simulations are performed for the PV panel model with different cell temperatures. The results are shown in Figure 7. These results from the model provide a great visual depiction of how small an effect a temperature change has when compared to a change in irradiance, shown in Figure 6. The Quasi-Double-Boost DC/DC Converter. The DC/DC converter is the next part of the system that needs to be tested. The converter tests are performed with a constant voltage source of 36 volts.

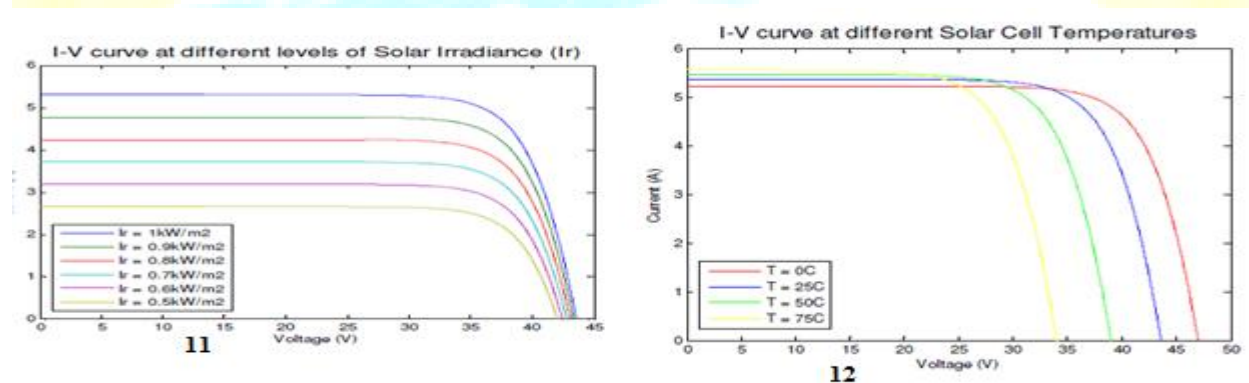
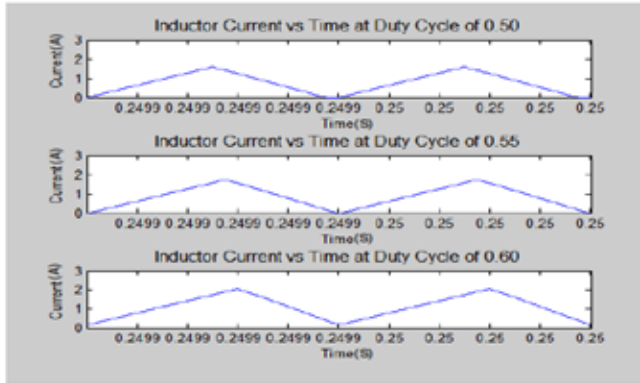


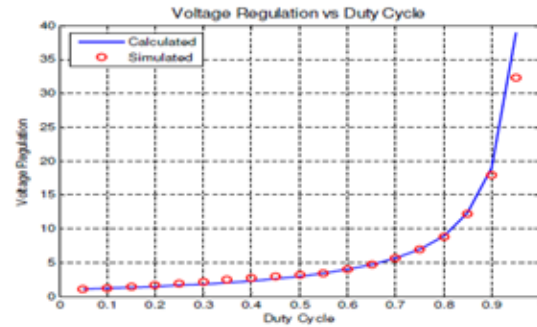
Figure 6. I-V curves at different levels of solar irradiance generated by the PV panel model. Figure 7. I-V curves at different levels of solar cell temperatures generated by the PV panel model.

This is both for ease of testing and for the accuracy of the results. Other system parameters are set as follows: the switching period of the converter is  $50 \mu\text{s}$  (20 kHz); the inductors are  $560 \mu\text{H}$  and the load resistance  $R$  is  $330 \Omega$ . The first aspect of the converter is its characteristics in different operating modes: CCM and DCM. This can be tested by looking at the inductor currents around the critical duty cycle found in equation (2-12). With the parameters set above and equation (2-12) it can be calculated that the critical duty cycle is 0.568. Figure 8 shows a converter duty cycle on each side of the critical value. From Figure 8 it is shown that when the duty cycle is 0.60, which is higher than the critical value the converter operates in CCM. The

figure also shows that when the duty cycle is lower than the critical value at 0.50, the converter operates in DCM. At a duty cycle of 0.55 which is close to the critical value but still below it the converter is only ever so slightly acting in DCM.



13



14

Figure 8. The inductor current of the converter in DCM and CCM, Figure 9. Comparison of the calculated and simulated results of voltage regulation for the DC/DC converter.

The next property of the converter to look at is the voltage regulation. To test voltage regulation the converter is ran at specific duty ratios while input and output voltages are measured. The regulation ratio is then compared to the ratio calculated by equation (2-15) in Figure 9. As is shown in the graph, the simulated results for the voltage regulation are close to what had been calculated. The one main difference is when the duty cycle is at 95%. At this point the simulated value is a gain of 32.4 while the calculated value is a gain of 39. This is believed to be due to the simulation being more accurate to real life where the higher voltage causes more losses through the components in the converter.

#### 4.2 The MPPT Control

The P&O MPPT method is implemented in Simulink and added to the converter circuit and PV panel model. The MPPT control unit takes as its input voltage and current measurements from the PV panel simulation. The control unit then computes the power and sends the information along with the PV panel voltage value into the P&O algorithm. The algorithm then decides whether the duty cycle output to the circuit should be increased, decreased or kept the same. This new duty cycle is then output to the converter. The process is able to hold the PV panel at its maximum power output under changing conditions. In order to test the MPPT control

algorithm the entire PV system has to be simulated. The best way to test the MPPT algorithm is by simulating the PV panel under various light conditions all while running the converter. This allows the tracking system to sense the changes in the panel output and correct for them using the duty cycle of the converter. Figure 10 shows the results of a 40 second simulation of the entire PV system. It can be seen that the irradiance was first increased from 0 to 1 kW/m<sup>2</sup> and then decreased back down to 0 in a stair step fashion. In the second part of Figure 10 the algorithm's reaction to the irradiance is shown in the form of the duty cycle it outputs. The third graph on Figure 10 shows the resulting solar power output from the panel.

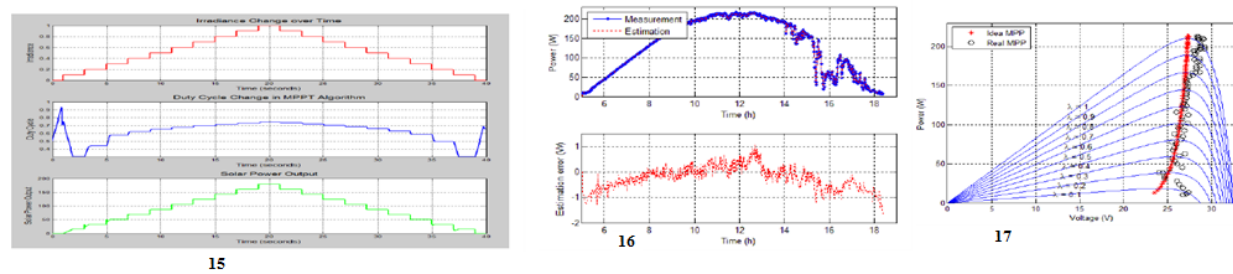


Figure 10. Simulation results of the MPPT control algorithm, Figure 11. The power estimation results, Figure 12. The MPPT results of the PV system.

There are a few interesting outcomes worth noting from the results shown in Figure 10. The first thing that is noticed is the rapid increase in the duty cycle at the beginning of the simulation. This is something that will only be seen in a simulation and is a result of the PV panel model being so accurate to real life. When a PV panel is not given any light at all it can actually work in a reverse. This is best described while talking about a panel hooked up to a battery directly. The reverse leakage current through the diodes within a solar cell can actually take power away from the battery and emit it through the PV panel when no light is present. The same is true for this simulation where the capacitor starts with a slight charge on it. The algorithm is actually doing exactly what it is supposed to, just backwards. When there is 0 kW/m<sup>2</sup> irradiance the PV panel model is actually taking power out of the capacitor and it is flowing backward through the circuit. Even though the amount of power is very small (~3e-30) the algorithm senses it and tries to compensate for it. This compensation is seen in Figure 10 by the duty cycle rapidly increasing at both the beginning and end of the simulation. Here the algorithm is actually trying to completely shut off the switches within the converter in order to lessen the loss of power. Since

the control algorithm only allows the converter to operate at a duty cycle from 5% to 95% when the duty cycle shown in Figure 10 increases to 95% it is reset at 72.5%. Shortly after this reset the irradiance increases to 0.1 kW/m<sup>2</sup>, which causes all backward power flow to cease. This allows the algorithm to settle at the duty cycle which allows the most power flow from the panel to the converter. There are two main reasons that the backward power flow seen in Figure 10 is only a simulation result. In the real system the controller will be powered from the PV panel in order to minimize losses when it is not needed. This means that when there is zero irradiance the controller will not be running and, therefore, the converter will already be in its off state, not allowing reverse power flow. The second reason this should not be seen in the real system is that there is almost never a time when there is absolutely no irradiance. At night the sun reflects off the moon, there are manmade lights everywhere and even the stars give off some irradiance that will be seen on the panel. While this isn't enough to see a usable amount of power, it is usually enough to stop the panel from allowing power to flow in reverse. The next thing to take notice of in Figure 10 is how good the system actually is at tracking the power output of the PV panel. At very low irradiance values the algorithm has a slight lag before it settles at the correct value since the duty cycle has to change so much. This can be seen both when the irradiance is increasing and when it is decreasing at values of 0.1 and 0.2 kW/m<sup>2</sup>. This is only seen at these low values and is almost completely eliminated at higher irradiance values. At the higher values of irradiance the algorithm is very quick at tracking to the new irradiance value once a change has occurred. With the simulation only being 40 seconds in total length and having irradiance changes in steps over the full range of values, the algorithm performed even better than expected. This shows that the algorithm should have no problem adjusting for a quickly changing MPP on partly cloudy days. The next step is to simulate the other current-sensorless technologies.

#### 4.3 Current-Sensorless MPPT Control

Simulation studies are carried out in MATLAB Simulink to validate the proposed current-sensorless MPPT quasi-double-boost converter for the PV system. These simulations are completed by using real solar radiation data obtained from National Renewable Energy Laboratory (NREL) to validate the proposed system and control algorithm. The data was collected from the South Table Mountain site in Golden, Colorado, on May 31, 2010. During the simulation, the output power of the PV panel is estimated by the proposed current-sensorless

MPPT algorithm and is compared with the measured output power by using both voltage and current transducers, as shown in the Figure 11. The proposed current-sensorless algorithm estimates the real output power with good precision; the estimation errors are less than 1 W during most of the day. Without knowing the solar radiation, the proposed MPPT algorithm controls the PV system to track the MPP of the PV panel by using the estimated current and measured voltage. Figure 12 shows the operating points, i.e., the real MPPs, of the panel at various solar radiation conditions during the day, which are close to ideal MPPs.

Inductor Current Sensing Technology Simulation studies are also carried out to validate the inductor current sensing

technology and the resulting MPPT control algorithm. These simulations were performed within MATLAB's Simulink using the neural network laid out as in Figure 10. The code for the neural network design can be seen in Appendix 2. In order to gather data to train the system, the converter simulation presented above was run again. The simulation used a varying duty cycle incremented in small steps and the resulting inductor voltage drop along with the input voltage and current were recorded. These results were then used to train the artificial neural network. The resulting mean square error (MSE) output from training can be seen in Figure 13, where the MSE is calculated by

$$MSE = \frac{1}{2} E^2 \quad \dots\dots 4.1$$

Where E is the error between the actual input current and the input current estimated by the artificial neural network.

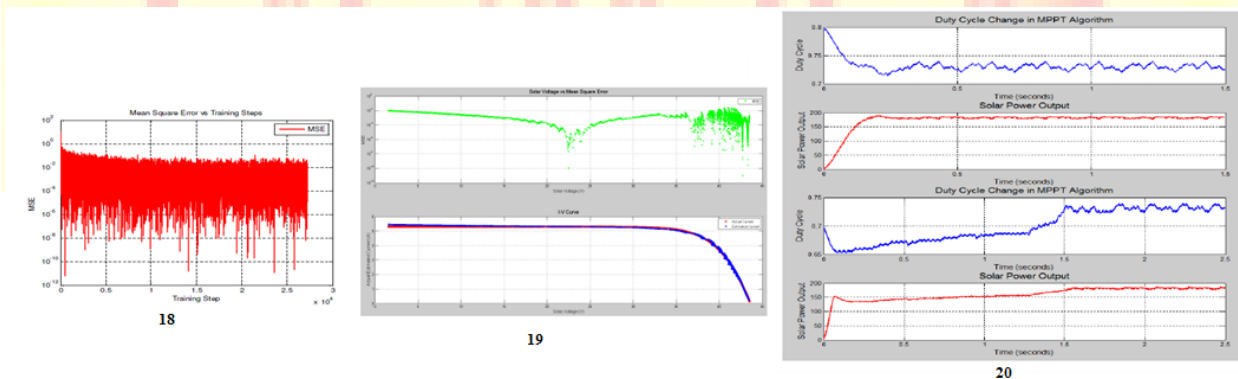




Figure 13. Mean square error output during the neural network training, Figure 14. Comparison of actual and estimated input current, Figure 15. Simulation results of the inductor sensing MPPT control algorithm.

Figure 13 shows that the mean square error stays below 10<sup>-1.5</sup> for all inputs by the end of the training period. To obtain a better understanding of what this actually means the weights found in testing, the neural network is applied to the data set recorded through the converter simulation and the estimated input current is compared against the actual recorded input current. The results of this comparison are shown in Figure 14.

Figure 14 shows the I-V curve output for both the estimated and the actual PV panel current. It can be seen that the two curves are very similar. While the two curves do not exactly match they are close enough to run the MPPT system. The important aspect of the curve for the MPPT algorithm is not the exact current value, but that the current is linear in the movement throughout the curve. The algorithm only cares whether the current is increasing or decreasing. This can further be seen by simulating the MPPT system while using the artificial neural network to estimate the input current within the algorithm. Figure 15 shows the results of running the system with the estimated current as an input to the MPPT algorithm. The irradiance is set to 1 kW/m<sup>2</sup> and the duty cycle is began to different values, one higher (80%) than the value expected for the maximum power output and one lower (70%). The algorithm finds the MPP in both directions to be 184 W, at a duty cycle of 74% which are the same as the results seen in Figure 10. When comparing the results after the algorithm has reached the MPP in Figure 15 and in Figure 10, it is again seen that they are the same. This shows that the algorithm with the inductor current sensing technology is working as good as the algorithm with the standard sensing technology, though it may be slightly slower. The inductor current sensing algorithm still manages to find both new MPP within 1.6 seconds. This is quick enough for the system to work under any normal working conditions. The next step was to apply the results observed in the simulation to the actual system.

#### 4.4 Sensing Technology Comparisons

All three of the sensing technologies work when simulated but each one has pros and cons when compared against each other. When comparing both current sensorless techniques there is not

really one that stands out over the other. Both work in the lower power application presented here but do not improve on the traditional resistor sense technology. Where the biggest improvement would be seen is in high power, high current applications. This is where the resistor sense technology would incur the most losses. However at these higher powers and currents the current sensorless and inductor current sense designs would not have any extra losses when compared to a low power system. Being used in a higher power system may even improve the accuracy of both systems. The higher current in the current sensorless design would give the system a more defined voltage ripple to perform calculations off of, improving overall results. The inductor current sense system would also have a higher inductor voltage drop to read into the neural network which would allow the system to obtain better accuracy in the current estimation. This would be due to there being a higher inductor voltage change correlated to the higher current. The higher current would however require retraining of the neural network to ensure proper operation. In low power applications with low current the standard resistor sense technology is recommended, both for ease of use, cost effectiveness, and reliability. In applications where the power level may change overtime, such as modular systems where panels may be added and removed the traditional system is also recommended. This is because both current sensorless technologies would have to be modified each time the input power level changed. With the traditional sense technology as long as the voltage drop across the resistance does not exceed the input rating of the voltage transducer used to measure it the system will continue to work without any modification at any power level. In higher power applications that would cause large power losses across a resistive element it is recommended that both the current sensorless and the inductor current sense technology be evaluated for performance with the overall system. High power applications are where these systems will excel over the traditional current sense technology.

## 5 CONCLUSIONS

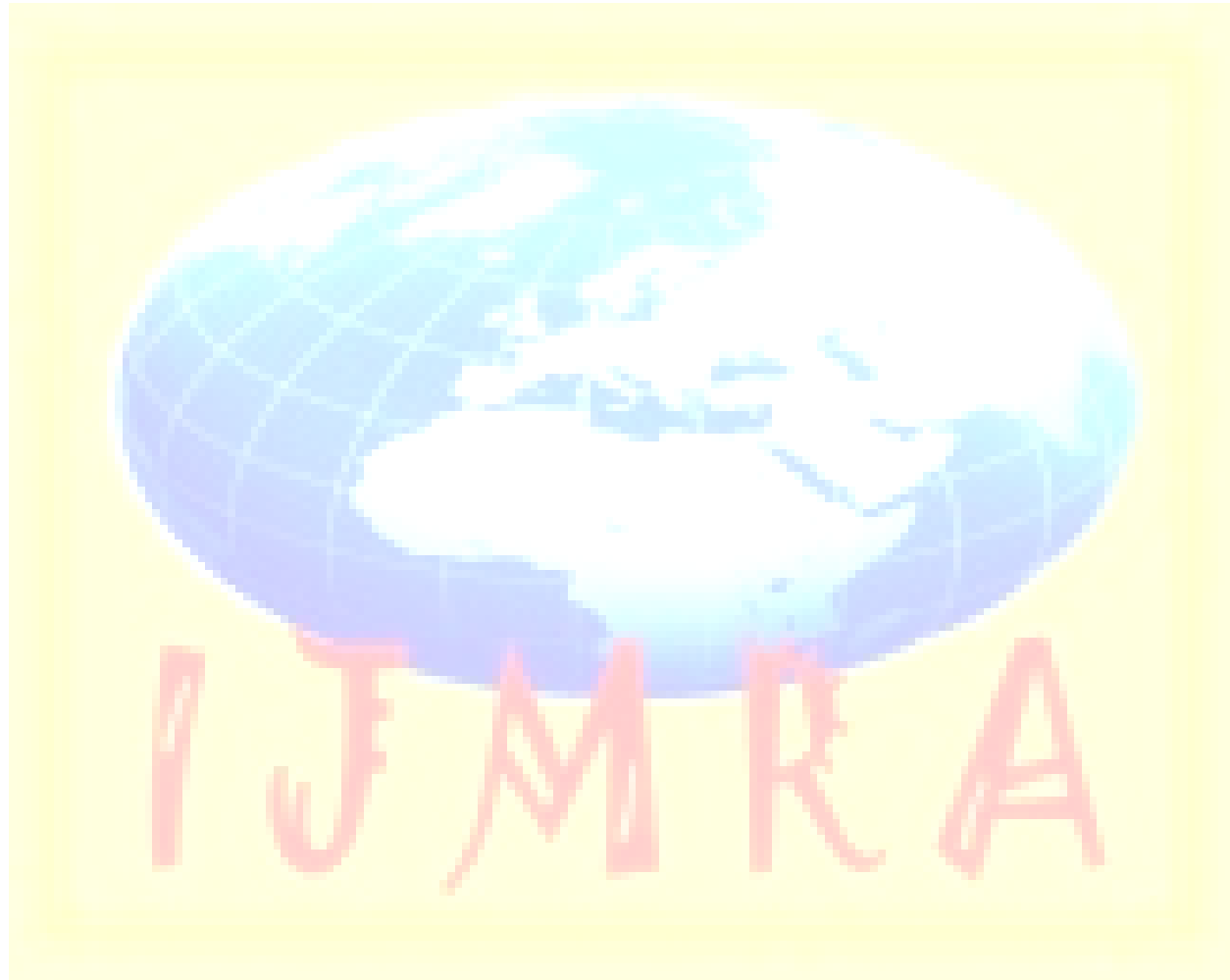
In order to maintain the highest power output from a PV panel at all times a high efficiency converter coupled with a MPPT system must be used. In this research a high efficiency quasi-double-boost DC/DC converter was designed and implemented. A fast reacting and accurate MPPT algorithm was implemented to control the converter and make sure the PV panel is always outputting the maximum power available at a given time. Results are presented showing the

output power improvement over a standard panel with a fixed load. Three separate current sensing and sensorless methods are presented to ensure the entire system operates with the highest possible efficiency. In future work it is recommended that all three current sensing technologies be implemented with identical converters and PV panels, so they can truly be tested against one another.

## 6. BIBLIOGRAPHY

1. Hua, C. (1998). Implementation of a DSP-Controlled Photovoltaic System with Peak Power Tracking. *IEEE Transactions on Industrial Electronics*, vol. 45, no. 1, 99-107.
2. Hussein, K. (1995). Maximum Photovoltaic Power Tracking: An Algorithm for Rapidly Changing Atmospheric Conditions. *IEE Proceedings Generation, Transmission and Distribution*, vol. 142, no. 1, 59-64.
3. Bernardo, P. C. (2009). A High Efficient Micro-controlled Buck Converter with Maximum Power Point Tracking for Photovoltaic Systems. *Proceedings of the International Conference on Renewable Energies and Power Quality*.
4. Lohmeier, C. (2011). A Current-Sensorless MPPT Quasi-Double-Boost Converter for PV Systems. *Proceedings of the 2011 IEEE Energy Conversion Congress and Exposition*, 1069-1075.
5. Mrabti, T. (2009). Regulation of Electric Power of Photovoltaic Generators With DC-DC Converter (Buck Type) and MPPT Command. *ICMCS '09. International Conference on Multimedia Computing and Systems*, 322-326.
6. Nabulsi, A. A. (2009). A 300 Watt Cascaded Boost Converter Design for Solar Energy Systems. *EPECS '09. International Conference on Electric Power and Energy Conversion Systems*, 1-4.
7. Orellana, M. (2010). Four Switch Buck-Boost Converter for Photovoltaic DC-DC Power Applications. *IECON 2010 - 36th Annual Conference on IEEE Industrial Electronics Society*, 469-474.
8. Pan, C. (1999). A Fast Maximum Power Point Tracker for Photovoltaic Power Systems. *Proceedings of the 25th Annual Conference of the IEEE Industrial Electronics Society Conference*, 390-393.

9. Rensburg, J. v. (2008). Double-Boost DC to DC Converter. Proceedings of the 34<sup>th</sup> Annual Conference of the IEEE Industrial Electronics Society Conference, 701-711.
10. Salas, V. (2006). Review of the Maximum Power Point Tracking Algorithms for Stand-Alone Photovoltaic Systems. Solar Energy Materials & Solar Cells, vol. 90, no. 11, 1555-1578.



## 6. ABOUT AUTHOR



**Mr. GANJI VIVEKANANDA**, Ph.D-Research Scholar at AcharyaNagarjuna University, Andhra Pradesh, India, And working as **Lecturer**, in the **Department of Electrical & Computer Engineering, College of Engineering & Tech, Aksum University**, Axum, Ethiopia and North East Africa. He studied **B.Tech (EEE)** from **CVSR Engineering college, JNTU, Hyderabad** and **M.Tech (Power Engineering and Energy Systems)** from, **J.N.T.U, Hyderabad, Telangana, India**. He is having 5+ years of work experience in **Academics, Teaching, and Industry & Research**. He participated and presented research papers in both national and international conferences, seminars and workshops; also published 5 research papers in national and international peer reviewed.



**Shri Mr. V KRISHNANAİK**, Ph.D - Research Scholar of **Mewar University**, Rajasthan,India.And Currently working as Assoc. Professor, in the Department of Electrical & Computer Engineering, College of Engineering & Tech, Aksum University, Ethiopia. He completed **B.E (ECE) from C.B.I.T, Osmania University, Hyderabad in 1999** and **M.Tech (Systems & Signal Processing) from J.N.U.C, J.N.T.U Hyderabad in 2005**. He is having 15+ years of relevant work experience in **Academics, Teaching, Industry & Research**. And utilizing his teaching skills, knowledge, experience and talent to achieve the goals and objectives of the Engineering College in the fullest perspective. He has attended more than 10 national and international conferences, seminars and workshops. He is also having to his credit more than 20 research articles and paper presentations which are accepted in national and international conference proceedings. His areas of Research in Digital signal processing, Image processing, speech processing, Digital Systems.